Enhanced channel estimation and symbol detection for high speed multi-input multi-output underwater acoustic communications

Jun Ling, Tarik Yardibi, Xiang Su, Hao He, and Jian Li[a)]
Department of Electrical and Computer Engineering, University of Florida, Gainesville, Florida 32611

(Received 2 August 2008; revised 11 February 2009; accepted 11 February 2009)

The need for achieving higher data rates in underwater acoustic communications leverages the use of multi-input multi-output (MIMO) schemes. In this paper two key issues regarding the design of a MIMO communications system, namely, channel estimation and symbol detection, are addressed. To enhance channel estimation performance, a cyclic approach for designing training sequences and a channel estimation algorithm called the iterative adaptive approach (IAA) are presented. Sparse channel estimates can be obtained by combining IAA with the Bayesian information criterion (BIC). Moreover, the RELAX algorithm can be used to improve the IAA with BIC estimates further. Regarding symbol detection, a minimum mean-squared error based detection scheme, called RELAX-BLAST, which is a combination of vertical Bell Labs layered space-time (V-BLAST) algorithm and the cyclic principle of the RELAX algorithm, is presented and it is shown that RELAX-BLAST outperforms V-BLAST. Both simulated and experimental results are provided to validate the proposed MIMO scheme. RACE'08 experimental results employing a 4×24 MIMO system show that the proposed scheme enjoys an average uncoded bit error rate of 0.38% at a payload data rate of 31.25 kbps and an average coded bit error rate of 0% at a payload data rate of 15.63 kbps. © *2009 Acoustical Society of America.* [DOI: 10.1121/1.3097467]

PACS number(s): 43.60.Fg, 43.60.Mn, 43.60.Ac [EJS] Pages: 3067–3078

I. INTRODUCTION

Achieving reliable communications with high data rates over underwater acoustic (UWA) channels has long been recognized as a challenging problem owing to the scarce bandwidth available and the double spreading phenomenon, i.e., spreading in both the time (delay spread) and frequency domains (Doppler spread).[1,2] Delay and Doppler spreading are inherent to many practical communication channels[3] but are profoundly amplified in underwater environments.[4–7]

The large spread in delay is the result of multipath propagation and the relatively low velocity of acoustic waves compared to electromagnetic waves.[2] When the delay spread is large, a transmitted symbol may interfere with many of its adjacent symbols at the receiver. This leads to severe intersymbol interference (ISI), which complicates the receiver structure and makes it difficult to extract the desired symbol from the measurements.

Doppler spreading stems from the random relative motion of the transmitters and receivers, and the nonstationarity of the underwater medium. This results in undesired phase shifts, making coherent communications using, for instance, phase-shift keying (PSK),[3] difficult for practical underwater communications. Thus, incoherent strategies, such as frequency-shift keying (FSK),[3] instead drew a lot of interest in the early UWA research.[8,9] Although being immune to double spreading, FSK is much less bandwidth efficient than PSK. After the employment of the phase locked loop (PLL) methodology[10,11] in underwater applications, coherent UWA communications gained popularity.[4,12,13]

While PLL is in general successful in mitigating the effects of Doppler spreading, the delay spread, or equivalently ISI, can be accounted for by either the decision feedback equalizer (DFE)[14,15] or the passive-phase conjugate[16] (PPC) methods. A detailed treatment alongside with performance comparisons of DFE and PPC is presented by Yang.[17,18] In practical UWA systems, the coupling of DFE and PLL has found great success[4,14] and almost became a standard.[6] DFE is a nonlinear equalizer, whose coefficients are updated by an adaptive approach such as the well-known recursive least squares (RLSs) or the least mean square algorithms.[4,19,20] The principle behind PPC is matched filtering, which states that when the channel impulse response (CIR) is convolved with its time-reversed and conjugated version at each receiver and added up, the summation approaches a delta function.[21] This compensates for the channel effects in the received signal. Obviously, the performance of such an approach relies heavily on the accuracy of the CIR estimate, especially when only few receivers exist. Taking one step further beyond the classic coupling of DFE with PLL, Yang[22] presented a hybrid structure combining the advantage of PPC with a single channel DFE and introduced a Doppler shift removal module before feeding the signals to the DFE.[23]

All the aforementioned methods, however, are confined to single-input multiple-output (SIMO) [or single-input single-output (SISO)] UWA communication systems. When multiple transmitters are used, interference between the multiple transmitted signals (besides ISI) degrades the perfor-

[a)]Author to whom correspondence should be addressed. Electronic mail: li@dsp.ufl.edu

mance of such methods significantly. This paper focuses on phase coherent communications over multi-input multi-output (MIMO) UWA channels with delay spreading only. We do not consider the effects of Doppler spreading herein. Yet, the methods presented in this paper can easily be extended to deal with Doppler spreading if desired.[24] The main motivation for establishing a MIMO system for underwater communications is the desire for higher data rates. As is well known, MIMO systems enjoy much higher data rates compared with their SIMO counterparts due to exploiting spatial diversity on both the receiver and the transmitter sides. To the best of our knowledge, there is not much work dealing with MIMO UWA communications in the literature. Early attempts[25,26] mainly focus on the design of the equalizer in the receiver end while some recent approaches[27,28] tackle the problem from a coding perspective. The design of a precoder that maps the source data to multiple transmitters in an optimal manner assuming that accurate channel estimates are available was presented by Kilfoyle *et al.*[29,30] In the present paper, we offer a broader view of the MIMO UWA communications problem and address two important issues: (i) estimation of the underwater CIR with delay spread and (ii) detection schemes for recovering the transmitted symbols using the estimated CIR.

In general, the very first task of the receiver is to conduct a training-directed channel estimation.[4,31] To achieve good performance, both well-structured training sequences and a signal processing methodology that can estimate the CIR accurately using the designed training sequences are required. In addition, to address the time-varying nature of the UWA channel, the decision-directed channel estimation is performed regularly using the detected symbols instead of the training symbols.[4,31] Therefore, the channel estimation algorithm should be able to work well both in training- and decision-directed modes.

When designing the training sequences, the delay spread of the UWA channel must be taken into account. For MIMO flat fading channels, i.e., channels without delay spread, Hadamard sequences[32,33] can be used effectively whereas for practical multipath channels, sequences with good auto- and cross-correlation properties instead are required.[34,35] Early research has focused on binary training sequences[34,36] due to practical concerns and simplicity. Later on, the use of polyphase training sequences was proposed, where the possible phase values were confined to a predefined finite set.[35] It is obviously advantageous to allow the phase values to be continuous. Yet, the problem becomes more demanding computationally as the degrees-of-freedom is allowed to increase. The cyclic approach (CA) presented by Li *et al.*[37,38] for probing sequence design enjoys superior performance over the aforementioned methods by allowing continuous phase values while still being computationally tractable. The training sequences designed using the CA methodology possess good auto- and cross-correlation properties as desired for MIMO channel estimation in communications.[37,38]

As mentioned previously, the second phase of channel estimation involves the design of the algorithm that will estimate the CIR using the training sequences (or the previously detected symbols) and highly contaminated measurements, be it either by the ISI and the interference from multiple transmitters or by the unpredictable nature of the underwater medium. Three important sparsity based techniques have been used for underwater channel estimation, namely, the matching pursuit (MP) algorithm, the orthogonal MP (OMP) algorithm,[39] and the least squares MP (LSMP) algorithm.[31,39–44] The main motivation for using MP type of algorithms is that many channels including underwater communication channels[14,45,46] and wireless channels are appropriately modeled as sparse channels consisting of a few dominant delay and Doppler taps.[47] One problem with these methods is that it is difficult to determine the stopping criterion and user intervention might be needed. Moreover, the performance of these methods might degrade significantly depending on the structure of the matrix relating the unknowns to the measurements. For instance, as will be shown in our numerical examples later on, these methods show better performance with CA designed training sequences rather than with arbitrary training sequences, especially when the training length is small. To address these problems, we present a user parameter-free nonparametric iterative adaptive approach[24] (IAA) for estimating the CIR accurately even when the training sequences are arbitrary and short in length. The dominant channel tap estimates of IAA can be used in a Bayesian information criterion (BIC)[48,49] to decide which taps to retain and which ones to discard. This combined method, called IAA with BIC, results in sparse channel estimates. Further improvements in performance can be achieved by initializing the last step of the cyclic and relaxation-based RELAX[50,51] algorithm via the IAA with BIC sparse estimates.

Following the estimation of the CIR is the design of the detection scheme for extracting the payload symbols from the measurements. We use a minimum mean-squared error (MMSE) based filter for signal detection. Two important methods for applying the MMSE filter coefficients to the measurements are the linear combinatorial nulling[52] (LCN) and vertical Bell Labs layered space-time (V-BLAST) algorithms.[53] It is interesting to note that these two approaches resemble the classical periodogram[54,55] and the CLEAN[56] methods used in spectral estimation applications. Being inspired from the improvements of RELAX over the periodogram and CLEAN,[54] we propose the RELAX-BLAST detection algorithm, which is a combination of V-BLAST and the cyclic principle of RELAX as the name suggests, and show that it outperforms V-BLAST.

The rest of this paper is organized as follows. Section II outlines the system configuration and describes the data package structure. Section III formulates the problem of CIR estimation, describes the CA method for training sequence design, and presents the IAA algorithm together with the BIC and RELAX extensions. Next, the symbol detection problem is analyzed in Sec. IV and the MMSE based RELAX-BLAST detection scheme is proposed. Both simulated and experimental results are presented in Sec. V. The sea data were gathered in the rescheduled acoustic communications experiment (RACE'08), which was conducted by the Woods Hole Oceanographic Institution (WHOI) in Narragansett Bay. This paper is concluded in Sec. VI.

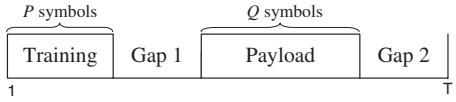

FIG. 1. The structure of a single data package.

The main contribution of the present paper is the thorough investigation of a MIMO UWA communications system by providing a detailed treatment of every step involved from data transmission to symbol detection at the receiver. This is done by presenting approaches for designing well-structured training sequences, a novel channel estimation method and a novel detection scheme. Simulation and experimental results validate the utility of the proposed overall scheme for MIMO underwater communications.

Notation: We denote vectors and matrices by boldface lowercase and boldface uppercase letters, respectively. $\|\cdot\|_2$ denotes the Euclidean norm, $\|\cdot\|_F$ denotes the Frobenius matrix norm, $(\cdot)^T$ denotes the transpose, $(\cdot)^H$ denotes the conjugate transpose, $E(\cdot)$ denotes the expected value, $\mathbf{I}$ denotes the identity matrix of appropriate size, and $\hat{\mathbf{x}}$ denotes the estimate of $\mathbf{x}$.

II. SYSTEM OUTLINE

Consider an $N\times M$ MIMO communications system equipped with N transmit transducers and M receive transducers. The individual data streams of each transmitter are symbol aligned and are sent simultaneously. The data streams of each transmitter consist of successive data packages of the form shown in Fig. 1. The data packages start with a training sequence of length P which is followed by a silent gap, the payload sequence, and another silent gap. During the gap intervals, no signal is transmitted in order to prevent the inner-package ISI (gap 1) between the training and payload symbols and the inter-package ISI (gap 2) between two consecutive packages. The payload sequence, which has length Q ($Q>P$ in general), is the estimation target and each payload symbol is drawn from a quadrature PSK (QPSK) constellation modulated with Gray code.[3] The four constellation points of the QPSK symbols, i.e., $\{e^{j(2n-1)\pi/4}\}_{n=1}^4$, lie on the unit circle. Such a constellation is desirable in practice due to its unit modulus. The same practical constraints require the training symbols to have unit modulus as well but no restriction is imposed on their phase values.

In what follows, our consideration is always confined to one data package of the form given in Fig. 1. Let $x_n(t)$ denote the tth symbol in the package sent by the nth transmitter and let $y_m(t)$ denote the tth symbol in the package received by the mth receiver, where $n=1,\ldots,N$, $m=1,\ldots,M$, $t=1,\ldots,T$, and T is the total symbol length of a single transmitted package. We do not go into the details of the sampling and synchronization procedures and assume that such operations have already been employed and the sampled complex baseband signals are available at the receiver.

Figure 2 shows the $N\times M$ MIMO system structure that we will use throughout the paper. The source bits are encoded, QPSK modulated, interleaved, and demultiplexed for transmission from multiple transducers. A random interleaver is used in order to avoid burst errors, which occur when the channel behaves badly at certain intervals of time.[3] After the signals have been received by the receive array, the processing consists of two steps: estimating the CIR (in training- or decision-directed mode) and detecting the symbols by using the estimated CIR. Once the symbols have been detected, they are multiplexed, deinterleaved, and then fed into a Viterbi decoder to recover the source bits. We now discuss the channel estimation problem.

III. CHANNEL ESTIMATION

In this section, we formulate the problem of channel estimation and describe the CA for training sequence design. We then propose IAA for channel estimation.

A. Problem formulation

1. Training-directed mode

The measurement vector at the mth receiver can be written as

$$\mathbf{y}_m=\sum_{n=1}^{N}\tilde{\mathbf{X}}_n\mathbf{h}_{n,m}+\mathbf{e}_m \tag{1}$$

for $m=1,\ldots,M$, where

$$\mathbf{y}_m=[y_m(1),\ldots,y_m(P+R-1)]^T, \tag{2}$$

$$\mathbf{h}_{n,m}=[h_{n,m}(1),\ldots,h_{n,m}(R)]^T, \tag{3}$$

and $R-1$ is the maximum number of delay taps under consideration. [Note that this corresponds to a $(R-1)\Delta t$ s delay spread, where Δt is the symbol interval.] $\mathbf{h}_{n,m}$ denotes the CIR between the nth transmitter and the mth receiver,

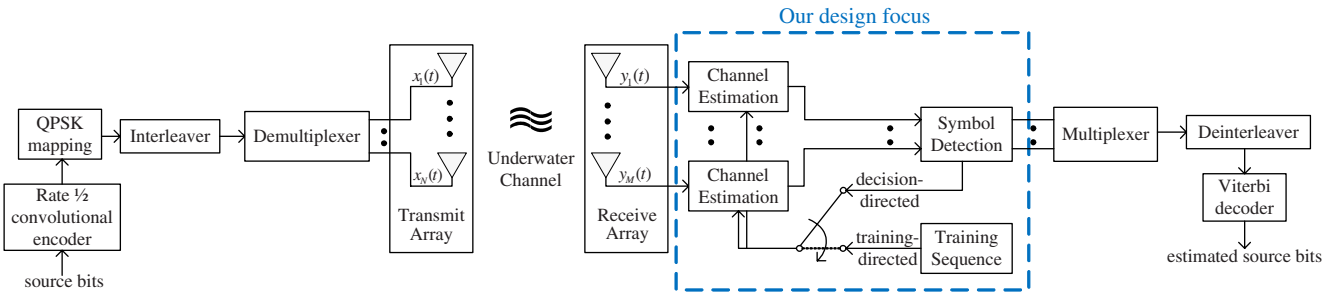

FIG. 2. (Color online) An $N\times M$ MIMO UWA communications system. The blocks inside the dashed rectangle are the focus of our attention in this paper.

$$\tilde{\mathbf{X}}_n = \begin{bmatrix} x_n(1) & \cdots & \mathbf{0} \\ \vdots & \ddots & \\ x_n(P) & & x_n(1) \\ & \ddots & \vdots \\ \mathbf{0} & \cdots & x_n(P) \end{bmatrix}, \tag{4}$$

where $\tilde{\mathbf{X}}_n \in \mathbb{C}^{(P+R-1)\times R}$ contains the nth training sequence and hence is known, and $\mathbf{e}_m$ is the additive noise (thermal or hardware related noise) at the mth receiver. Equation (1) can be rewritten as

$$\mathbf{y}_m = \mathbf{X}\mathbf{h}_m + \mathbf{e}_m, \tag{5}$$

where $\mathbf{X}=[\tilde{\mathbf{X}}_1 \cdots \tilde{\mathbf{X}}_N]$ and $\mathbf{h}_m=[\mathbf{h}_{1,m}^T \cdots \mathbf{h}_{N,m}^T]^T$. The training-directed channel estimation problem then reduces to estimating $\mathbf{h}_m$ from the measurements $\mathbf{y}_m$ and known $\mathbf{X}$. It is assumed that the channel is stationary over the length of $\mathbf{y}_m$. In order to estimate all the channels for the $N\times M$ MIMO system, Eq. (5) has to be solved for $m=1,\ldots,M$, i.e., M times. Note that $\mathbf{X}$ does not depend on m.

2. Decision-directed mode

The problem in the decision-directed mode is very similar to that of the training-directed mode except that now the training symbols are replaced with the previously estimated payload symbols. Consequently, Eq. (5) can be expressed as

$$\mathbf{y}_m = \hat{\mathbf{X}}\mathbf{h}_m + \mathbf{e}_m, \tag{6}$$

where $\hat{\mathbf{X}}=[\hat{\mathbf{X}}_1 \cdots \hat{\mathbf{X}}_N]$,

$$\hat{\mathbf{X}}_n = \begin{bmatrix} \hat{x}_n(t_i) & \hat{x}_n(t_i-1) & \cdots & \hat{x}_n(t_i-R+1) \\ \hat{x}_n(t_i+1) & \hat{x}_n(t_i) & \cdots & \hat{x}_n(t_i-R+2) \\ \vdots & \vdots & & \vdots \\ \hat{x}_n(t_f) & \hat{x}_n(t_f-1) & \cdots & \hat{x}_n(t_f-R+1) \end{bmatrix}, \tag{7}$$

$$\mathbf{y}_m = [y_m(t_i), \ldots, y_m(t_f)]^T, \tag{8}$$

and where $\hat{x}_n(t_i-R+1)$ and $\hat{x}_n(t_f)$ represent the first and the last previously estimated symbols, respectively, used for updating the channel. The decision-directed channel estimation problem reduces to estimating $\mathbf{h}_m$ from the measurements $\mathbf{y}_m$ and the previously decoded symbols in $\hat{\mathbf{X}}$.

On the one hand, it would be beneficial to keep $L \triangleq t_f - t_i + R$ large for estimating the channel more accurately but on the other hand, for a rapidly varying channel, L must be kept small so that the stationarity assumption of the channel over the length of $\mathbf{y}_m$ holds and so that the channel can be updated more frequently. Therefore, L is a trade-off parameter which should be set according to the experimental conditions.

Note that the channel estimates obtained using the training sequences may become outdated before the first set of payload symbols are estimated due to the gap between the training and payload sequences. However, the length of the gap interval is relatively small and this effect can often be neglected. If the sea is expected to be very nonstationary, a smaller gap interval should be used even though this will increase the ISI between the training and the payload sequences.

B. Training sequence design

We use the algorithm presented by Li *et al.*[37,38] for designing training sequences such that $\mathbf{X}$ in Eq. (5) facilitates the estimation of the CIR. It is desirable to have training symbols with constant modulus, i.e., the training symbols should have the following generic form:

$$x_n(t) = e^{j\phi_n(t)}, \quad t=1,\ldots,P, \quad n=1,\ldots,N, \tag{9}$$

where $\phi_n(t) \in [0, 2\pi)$ represents the phase of the tth training symbol sent by the nth transmitter. Ideally, if $\mathbf{X}^H\mathbf{X}=P\mathbf{I}$ (called the pairwise orthogonality principle), then the channel estimates can be recovered perfectly by matched filtering in the noiseless case. However, pairwise orthogonality is hardly achievable, if not impossible, in practice.[38] Instead, $\epsilon=\|\mathbf{X}^H\mathbf{X}-P\mathbf{I}\|_F^2$ can be made small.

Let $\mathbf{U}$ be an arbitrary semi-unitary matrix (i.e., $\mathbf{U}\mathbf{U}^H=\mathbf{I}$). Then,

$$\epsilon = \|\mathbf{X}^H\mathbf{X} - (\sqrt{P}\mathbf{U})(\sqrt{P}\mathbf{U}^H)\|_F^2. \tag{10}$$

Minimizing ϵ can then be formulated in the following related (but not equivalent) way:[38]

$$\{\phi_n(t)\} = \underset{\{\phi_n(t)\},\mathbf{U}^H}{\operatorname{argmin}} \|\mathbf{X} - \sqrt{P}\mathbf{U}^H\|_F^2, \quad \text{subject to } \mathbf{U}\mathbf{U}^H = \mathbf{I}. \tag{11}$$

This optimization problem can be solved efficiently by using the CA method[38,57] which guarantees that the cost function does not increase as the iterations proceed. In the CA method, $\mathbf{U}$ is assumed given when estimating $\{\phi_n(t)\}$ and vice versa. This way, the optimization problem is solved iteratively by dividing it into simpler sub-problems.

When $\mathbf{U}^H$ is fixed, the solution to Eq. (11) has the generic form

$$\phi = \arg\left(\sum_{r=1}^{R} z_r\right), \tag{12}$$

where $\{z_r\}_{r=1}^R$ are given numbers. For example, when the update target is $\phi_1(1)$, z_r represents the (r,r)th diagonal entry of $\sqrt{P}\mathbf{U}^H$.

Given the phases $\phi_n(t)$, the solution to Eq. (11) is given by $\mathbf{U}^H=\bar{\mathbf{U}}\tilde{\mathbf{U}}^H$,[38,58] where

$$\sqrt{P}\mathbf{X} = \bar{\mathbf{U}}\mathbf{\Gamma}\tilde{\mathbf{U}}^H \tag{13}$$

is the singular value decomposition of $\sqrt{P}\mathbf{X}$ ($\bar{\mathbf{U}}$ and $\tilde{\mathbf{U}}^H$ are unitary matrices and $\mathbf{\Gamma}$ is a diagonal matrix with the singular values of $\sqrt{P}\mathbf{X}$ on its diagonal).

The CA algorithm is terminated when the difference of the cost function [defined in Eq. (11)] between two successive iterations drops below a certain threshold. For the CA algorithm to show good performance, it is recommended that $P \gg R$ and $NR < P+R-1$.[37,38] In practice, N is determined from the system configuration while R is selected depending on the experimental conditions and is expected to be the

smallest value that can capture the prominent channel features. It seems as if a large P value is preferable for satisfying the two inequalities. However, there are two problems associated with increasing P. First, the accuracy of the initial channel estimation depends on the assumption that the channel is stationary. For a fixed symbol rate, larger P means longer transmission time which means the stationarity assumption is more likely to be violated. Second, larger P means larger overhead and hence lower net data rate. Fortunately, though, the two inequalities can in general be satisfied in practice by selecting the parameters appropriately. Note that the CA method has been used to design the training sequences in Sec. V of this paper.

C. The channel estimation algorithm: IAA

The channel estimation problem at each receiver has the generic form given by [see Eqs. (5) and (6)]

$$\mathbf{y} = \mathbf{S}\mathbf{h} + \mathbf{e}, \tag{14}$$

where we have omitted the index m and replaced $\mathbf{X}$ (for the training-directed mode) or $\hat{\mathbf{X}}$ (for the decision-directed mode) by $\mathbf{S}$ for notational simplicity. Note that the number of elements in $\mathbf{y}$, namely, d_y, is also different for the two modes. The problem is then to estimate $\mathbf{h}$, which has NR unknowns, given $\mathbf{y}$ and $\mathbf{S}$. In the following, we present the IAA algorithm[24] to solve this problem. IAA makes no assumptions on the statistical properties of the additive noise $\mathbf{e}$. Note that since $\mathbf{h}$ contains the CIR of all N transmitters, IAA will estimate them jointly.

1. IAA

Many existing weighted least squares (WLSs) based channel estimation methodologies require the tuning of one or more user parameters and their assumptions on the CIR are in general not valid in the underwater scenario.[59,60] To account for these problems, we present a user parameter-free iterative WLS based channel estimation technique, called IAA.[24] IAA is an adaptive and nonparametric algorithm, and it does not make any explicit assumptions on the CIR. Let $\mathbf{P}$ be an $NR \times NR$ diagonal matrix whose diagonal contains the squared absolute value of each channel tap, i.e.,

$$P_r = |h_r|^2, \quad r = 1, \ldots, NR, \tag{15}$$

where P_r is the rth diagonal element of $\mathbf{P}$ and h_r is the rth element of $\mathbf{h}$. If the rth column of $\mathbf{S}$ is written as $\mathbf{s}_r$, then the covariance matrix of the noise and interference with respect to the tap of current interest h_r can be expressed as

$$\mathbf{Q}(r) = \mathbf{R} - P_r \mathbf{s}_r \mathbf{s}_r^H, \tag{16}$$

where $\mathbf{R} \triangleq \mathbf{S}\mathbf{P}\mathbf{S}^H$. Then, the WLS cost function is given by[54,61–63]

$$(\mathbf{y} - h_r \mathbf{s}_r)^H \mathbf{Q}^{-1}(r)(\mathbf{y} - h_r \mathbf{s}_r). \tag{17}$$

Minimizing Eq. (17) with respect to h_r yields

TABLE I. IAA.

$P_r = \dfrac{|\mathbf{s}_r^H \mathbf{y}|^2}{(\mathbf{s}_r^H \mathbf{s}_r)^2}$, $r = 1, 2, \ldots, NR$
repeat
  $\mathbf{R} = \mathbf{S}\mathbf{P}\mathbf{S}^H$
  $\hat{h}_r = \dfrac{\mathbf{s}_r^H \mathbf{R}^{-1} \mathbf{y}}{\mathbf{s}_r^H \mathbf{R}^{-1} \mathbf{s}_r}$, $r = 1, 2, \ldots, NR$
  $P_r = |\hat{h}_r|^2$, $r = 1, 2, \ldots, NR$
until (convergence)

$$\hat{h}_r = \frac{\mathbf{s}_r^H \mathbf{Q}^{-1}(r) \mathbf{y}}{\mathbf{s}_r^H \mathbf{Q}^{-1}(r) \mathbf{s}_r}. \tag{18}$$

Using Eq. (16) and the matrix inversion lemma, Eq. (18) can be written as

$$\hat{h}_r = \frac{\mathbf{s}_r^H \mathbf{R}^{-1} \mathbf{y}}{\mathbf{s}_r^H \mathbf{R}^{-1} \mathbf{s}_r}. \tag{19}$$

This avoids the computation of $\mathbf{Q}^{-1}(r)$ for NR times and only one matrix inversion is needed per iteration. IAA for channel estimation is summarized in Table I. Since IAA requires $\mathbf{R}$, which itself depends on the unknown channel taps, it has to be implemented as an iterative approach. The initialization is done by a standard matched filter. Our empirical experience is that IAA does not provide significant improvements in performance after about 15 iterations. In IAA, $\mathbf{P}$ and hence $\mathbf{R}$ are obtained from the channel estimates of the previous iteration and not from the measurements $\mathbf{y}$ as done in conventional adaptive filtering algorithms.

If the computation of $\mathbf{R}$ becomes problematic due to numerical ill-conditioning during the iterations, a regularization approach can be used. IAA can be regularized by considering an additional noise term separately from the interference terms in the expression for $\mathbf{R}$:

$$\mathbf{R} = \mathbf{S}\mathbf{P}\mathbf{S}^H + \mathbf{\Sigma}, \tag{20}$$

where $\mathbf{\Sigma}$ is a diagonal matrix with unknown noise powers $\{\sigma_m^2\}_{m=1}^{d_y}$ on its diagonal. IAA is then implemented in the same way as before except that now there are $NR + d_y$ rather than NR unknowns. Consequently, $\{\sigma_m^2\}$ can be estimated by

$$\hat{\sigma}_m^2 = \frac{|\mathbf{i}_m^H \mathbf{R}^{-1} \mathbf{y}|^2}{(\mathbf{i}_m^H \mathbf{R}^{-1} \mathbf{i}_m)^2}, \quad m = 1, \ldots, d_y, \tag{21}$$

at each iteration, where $\mathbf{i}_m$ is the mth column of the $d_y \times d_y$ identity matrix. Since the diagonal loading levels are calculated automatically, the approach conserves the practicality of IAA. Setting $\{\hat{\sigma}_m\}_{m=1}^{d_y}$ to zero gives the original IAA algorithm. $\mathbf{\Sigma}$ can be initialized as all zeros.

2. IAA with BIC

In order to achieve sparsity with IAA, i.e., to retain only a few dominant channel taps, the BIC[48,49] can be used in conjunction with IAA. BIC is a model order selection tool that is widely used in the statistics and signal processing communities. The advantage of using BIC over a simple thresholding operation is that BIC does not require the manual specification of a threshold value. (Note that the se-

TABLE II. IAA with BIC.

$\mathcal{P}=\{1,\ldots,NR\}$
$\mathcal{I}=\{\varnothing\}$; $\eta=1$; quit=0; $\mathrm{BIC}^{\mathrm{old}}=\infty$
repeat
  $i'=\mathrm{argmin}_{i\in\mathcal{P}-\mathcal{I}}\mathrm{BIC}_i(\eta)$
  if $\mathrm{BIC}_{i'}(\eta)<\mathrm{BIC}^{\mathrm{old}}$
    $\mathcal{I}=\{\mathcal{I},i'\}$
    $\mathrm{BIC}^{\mathrm{old}}=\mathrm{BIC}_{i'}(\eta)$
    $\eta=\eta+1$
  else quit=1
until (quit=1)

lection of the threshold value has a significant effect on the overall performance and it is usually impractical to tune this value for best performance since the true CIR is unknown.) Let $\mathcal{P}$ denote a set containing the indices of all the channel taps. Also, let $\mathcal{I}$ denote the set of the indices of the taps selected by the BIC algorithm so far. The IAA with BIC algorithm works as follows: first, the tap from the set $\mathcal{P}$ giving the minimum BIC is selected and included in the set $\mathcal{I}$ (initially $\mathcal{I}=\varnothing$). Then the second tap, from the set $\mathcal{P}-\mathcal{I}$, which together with the first tap gives the minimum BIC is selected and so on until the BIC value does not decrease anymore. The IAA with BIC algorithm is summarized in Table II. $\mathrm{BIC}_i(\eta)$ is calculated as follows:[48]

$$\mathrm{BIC}_i(\eta)=2d_y\ln\left(\left\|\mathbf{y}-\sum_{j\in\{\mathcal{I}\cup i\}}\mathbf{s}_j\hat{h}_j\right\|_2^2\right)+1.5\,\eta\ln(2d_y), \tag{22}$$

where $\eta=|\mathcal{I}|+1$, with $|\mathcal{I}|$ denoting the size of $\mathcal{I}$, i is the index of the current tap under consideration, and $\hat{h}_j$ is the IAA estimate of the jth element of $\mathbf{h}$, $j\in\{\mathcal{I}\cup i\}$. After BIC is implemented, the indices of the surviving CIR taps can be found in $\mathcal{I}$. All other channel taps are then set to zero.

3. IAA with RELAX

The parametric and cyclic RELAX algorithm,[50,51] which was originally proposed for spectral estimation, can be used to improve the IAA with BIC results even further. Because RELAX is parametric, it requires the number of sources to be known. The IAA with BIC result can be used to estimate the number of sources and also to provide initial estimates for the last step of RELAX, as shown in Table III. Note that $\mathcal{I}(k)$ denotes the kth element in the set $\mathcal{I}$. The idea presented in Table III is to remove the contribution from all the components of $\hat{\mathbf{h}}$ other than the one of current interest $\hat{h}_{\mathcal{I}(k)}$ and then to update $\hat{h}_{\mathcal{I}(k)}$ in the minimum least squares sense. This procedure is repeated until the difference of the cost function $\|\mathbf{y}-\mathbf{S}\hat{\mathbf{h}}\|_2^2$ between two successive iterations becomes less than a certain threshold. (We used a threshold of 5×10^{-3} in our simulations herein.) For the best performance, it is recommended that before each RELAX iteration, $\{\hat{h}_k\}$ be sorted by their magnitude in descending order and the columns of $\mathbf{S}$ be permuted accordingly. This way, the tap with the largest magnitude will be updated first, the tap with the second largest magnitude will be updated next, and so on.

TABLE III. IAA with RELAX.

$\mathcal{I}$: Indices of the taps selected by IAA with BIC
$K=|\mathcal{I}|$, i.e., the number of selected taps
repeat
  for $k=1,2,\ldots,K$
    $\mathbf{y}_k=\mathbf{y}-\sum_{i=1,i\neq k}^{K}\mathbf{s}_{\mathcal{I}(i)}\hat{h}_{\mathcal{I}(i)}$
    $\hat{h}_{\mathcal{I}(k)}=\mathbf{s}_{\mathcal{I}(k)}^H\mathbf{y}_k/\|\mathbf{s}_{\mathcal{I}(k)}\|_2^2$
  end for
until (convergence)

4. Complexity analysis

The initialization step of IAA has complexity $\mathcal{O}(2d_y(NR)+3(NR))$ and each IAA iteration has complexity $\mathcal{O}(d_y^3+(2d_y^2+3d_y+2)(NR))$. These complexities are calculated by counting the multiplication and division operations in Table I. When $d_y>(NR)$, $\mathbf{R}^{-1}$ can be calculated only once at the initialization step of IAA and then it can be updated when every $\{P_r\}$ is estimated using the rank-1 matrix inverse update formula.[64] This way, the complexity of computing $\mathbf{R}^{-1}$ reduces to $\mathcal{O}((d_y^2+3)(NR))$ rather than $\mathcal{O}(d_y^3)$ at each IAA iteration. The resulting complexity of IAA is then given by $\mathcal{O}(d_y^3+(d_y^2+3d_y+3)(NR))$ for initialization and $\mathcal{O}((2d_y^2+2d_y+5)(NR))$ per IAA iteration. The complexity of IAA is smaller than those of MP and LSMP when $d_y\ll(NR)$ and larger when $d_y>(NR)$.[31] However, the computation time does not depend only on the number of computations but rather is a function of the memory access time, the implementation software and hardware, and the number of computations combined together.

Note that the regularization, BIC, and RELAX extensions will be applied in all of our numerical examples and henceforth this combined approach will simply be referred to as IAA.

IV. SYMBOL DETECTION

The symbol detection problem is to estimate the transmitted payload symbols using the CIR estimates. In this section we first describe how to obtain the MMSE filter coefficients for each symbol of interest and then describe three methods on how to apply these filter coefficients to the measurements.

A. Problem formulation

Once the CIR estimates are available, the transmitted symbols can be detected by expressing Eq. (6) as[15]

$$\mathbf{y}_m=\tilde{\mathbf{H}}_m\tilde{\mathbf{x}}+\mathbf{e}_m, \tag{23}$$

where

$$\mathbf{y}_m=[y_m(t_0),\ldots,y_m(t_0+R-1)]^T, \tag{24}$$

t_0 represents the index corresponding to the payload symbol that is to be detected, $\tilde{\mathbf{H}}_m=[\hat{\mathbf{H}}_{1,m}\cdots\hat{\mathbf{H}}_{N,m}]$,

$$\hat{\mathbf{H}}_{n,m} = \begin{bmatrix} \hat{h}_{n,m}(R) & \cdots & \hat{h}_{n,m}(1) & & \mathbf{0} \\ \vdots & \ddots & & \ddots & \vdots \\ \mathbf{0} & & \hat{h}_{n,m}(R) & \cdots & \hat{h}_{n,m}(1) \end{bmatrix}, \tag{25}$$

$\tilde{\mathbf{x}} = [\mathbf{x}_1^T \cdots \mathbf{x}_N^T]^T$, and

$$\mathbf{x}_n = [x_n(t_0 - R + 1), \ldots, x_n(t_0), \ldots, x_n(t_0 + R - 1)]^T. \tag{26}$$

Note that $\mathbf{y}_m$ is used to represent the measurements in Eqs. (5), (6), and (23) since $\mathbf{y}_m$ represents a portion of the received signal in any case. However, the use of $\mathbf{y}_m$ should be clear from the context. When detecting the symbols, the channel is assumed to be stationary, which allows keeping $\tilde{\mathbf{H}}_m$ in Eq. (23) constant.

If the measurements from all the receivers are stacked up together, we obtain

$$\begin{bmatrix} \mathbf{y}_1 \\ \mathbf{y}_2 \\ \vdots \\ \mathbf{y}_M \end{bmatrix} = \begin{bmatrix} \tilde{\mathbf{H}}_1 \\ \tilde{\mathbf{H}}_2 \\ \vdots \\ \tilde{\mathbf{H}}_M \end{bmatrix} \tilde{\mathbf{x}} + \begin{bmatrix} \mathbf{e}_1 \\ \mathbf{e}_2 \\ \vdots \\ \mathbf{e}_M \end{bmatrix} \tag{27}$$

or

$$\tilde{\mathbf{y}} = \tilde{\mathbf{H}}\tilde{\mathbf{x}} + \tilde{\mathbf{e}}. \tag{28}$$

The transmitted symbols $\{x_n(t_0)\}$ are estimated using Eq. (28). When estimating $\{x_n(t_0+1)\}$, the measurement vector $\tilde{\mathbf{y}}$ is shifted by one symbol duration and so on. Yet, $\tilde{\mathbf{H}}$ remains constant since the channel is assumed to be stationary during the process.

B. The MMSE filter

In this section, we briefly review the Wiener filter,[65,66] which is optimal in the MMSE sense with respect to each transmitted symbol, for symbol detection. The Wiener filter is widely used in the communication literature[53,67,68] and the exposition provided in this section is for the sake of completeness. The steering vector corresponding to $\{x_n(t_0)\}$ in Eq. (28) is given by $\mathbf{d}_n \triangleq [\hat{\mathbf{h}}_{n,1}^T \cdots \hat{\mathbf{h}}_{n,M}^T]^T$, where $\hat{\mathbf{h}}_{n,m}$ are the estimates of $\mathbf{h}_{n,m}$ defined in Eq. (3). We let the symbol of current interest be $x_n(t_0)$. Then, the Wiener filter for this symbol, denoted as $\mathbf{g}_n$, can be derived by solving

$$\mathbf{g}_n = \underset{\mathbf{g}}{\operatorname{argmin}}\, E(\|\mathbf{g}^H\tilde{\mathbf{y}} - x_n(t_0)\|_2^2). \tag{29}$$

The solution to Eq. (29) is[65,66]

$$\mathbf{g}_n = \mathbf{R}_{\tilde{\mathbf{y}}\tilde{\mathbf{y}}}^{-1} E(x_n^H(t_0)\tilde{\mathbf{y}}), \tag{30}$$

where $\mathbf{R}_{\tilde{\mathbf{y}}\tilde{\mathbf{y}}}$ is the covariance matrix of $\tilde{\mathbf{y}}$, i.e., $\mathbf{R}_{\tilde{\mathbf{y}}\tilde{\mathbf{y}}} = E(\tilde{\mathbf{y}}\tilde{\mathbf{y}}^H)$.

In the following, it is assumed that the payload sequences are pairwise uncorrelated, each payload sequence is uncorrelated with the noise $\tilde{\mathbf{e}}$, the noise has zero mean, each payload symbol is independent of the other payload symbols, and each payload symbol has zero mean. These assumptions can be stated mathematically as follows:

$$E(\tilde{\mathbf{x}}\tilde{\mathbf{x}}^H) = \mathbf{I}, \quad E(\tilde{\mathbf{x}}\tilde{\mathbf{e}}^H) = \mathbf{0}. \tag{31}$$

Using Eqs. (28) and (31), we obtain

$$\mathbf{R}_{\tilde{\mathbf{y}}\tilde{\mathbf{y}}} = \tilde{\mathbf{H}}\tilde{\mathbf{H}}^H + \mathbf{R}_{\tilde{\mathbf{e}}\tilde{\mathbf{e}}} \tag{32}$$

and $E(x_n^H(t_0)\tilde{\mathbf{y}}) = \mathbf{d}_n$. Equation (30) then becomes

$$\mathbf{g}_n = (\tilde{\mathbf{H}}\tilde{\mathbf{H}}^H + \mathbf{R}_{\tilde{\mathbf{e}}\tilde{\mathbf{e}}})^{-1}\mathbf{d}_n, \tag{33}$$

and the soft estimate of the symbol $x_n(t_0)$ is given by $\mathbf{g}_n^H\tilde{\mathbf{y}}$. In our experiments we estimate $\mathbf{R}_{\tilde{\mathbf{e}}\tilde{\mathbf{e}}}$ from the residual error obtained during the channel estimation process, i.e., using $\mathbf{e}_m = \mathbf{y}_m - \mathbf{S}\hat{\mathbf{h}}_m$, $m = 1, \ldots, M$, in Eq. (14). Since digital communications require the receiver to make a hard decision, the nearest constellation point to $\mathbf{g}_n^H\tilde{\mathbf{y}}$ is selected as the symbol estimate.

C. Detection schemes

In the following, we will consider three approaches for applying the filters $\{\mathbf{g}_n\}$ to the measurements. We will note the relations between the approaches proposed in the communications literature with those in the spectral estimation area and propose a new scheme inspired by this relationship.

1. Linear combinatorial nulling (LCN)

In LCN,[52] $x_n(t_0)$ is detected using $\mathbf{g}_n^H\tilde{\mathbf{y}}$ for $n = 1, \ldots, N$ separately where for each n, other symbols are simply treated as interferences, i.e., the estimation of $x_n(t_0)$ has no effect on the estimation of $x_{n'}(t_0)$ $(n' \neq n)$. However, this approach shows poor performance when the channel coefficients for each transmitter differ significantly in magnitude. For instance, when the channel coefficients of the first transmitter dominate all the others, the symbol estimate for the first transmitter will be relatively accurate whereas the symbols sent from the other transmitters will be buried under the contribution from the first transmitter and hence they will be estimated inaccurately.

2. CLEAN-BLAST

The idea of sequential cancellation and nulling (SCN) can be used to alleviate the aforementioned drawback of LCN. As the name implies, SCN first detects the symbol with the strongest channel response. Then, the contribution of this symbol is removed from the measurements $\tilde{\mathbf{y}}$ (and the corresponding columns are removed from $\tilde{\mathbf{H}}$) before estimating the other symbols. This process continues until all the N symbols are estimated. The symbol with the strongest channel coefficients is detected first because it can be estimated more accurately than the other symbols with weaker channel coefficients. After the dominant symbols are subtracted from the measurements, the weaker symbols can be estimated more accurately. Sequential cancellation, from the viewpoint of the remaining symbols, can be recognized as interference removal. Eventually, when detecting the symbol with the weakest channel coefficients, no more interferences are present. The detection algorithm featuring SCN is called V-BLAST.[53] Herein, we name the algorithm as CLEAN-BLAST to emphasize its analogy to the CLEAN algorithm used in spectral estimation.[69]

3. RELAX-BLAST

As we have already pointed out, the relationship between LCN and CLEAN-BLAST is analogous to that of the periodogram and CLEAN.[54] In spectral estimation, RELAX is also called SUPER-CLEAN[50,51] since it is a recursive version of CLEAN but with much better performance. In the same spirit as RELAX, RELAX-BLAST first detects the symbol with the dominant channel taps and subtracts it out from $\tilde{\mathbf{y}}$. Then, it estimates the next dominant symbol from the residue signal. Unlike CLEAN-BLAST, however, which at this time estimates the third strongest symbol, RELAX-BLAST instead updates the two already detected symbols in an iterative manner until the difference of the RELAX-BLAST estimates between two successive iterations becomes less than a certain threshold. Once these two symbols are subtracted from the measurements and the third strongest symbol is estimated, the three symbols are again updated in an iterative manner until all the three estimates do not improve anymore. This process is repeated until all the N symbols are detected and updated.

Finally, note that when $N=1$, i.e., for a SIMO or SISO system, LCN, CLEAN-BLAST, and RELAX-BLAST become identical approaches.

V. NUMERICAL AND EXPERIMENTAL RESULTS

In this section we evaluate the performance of the CA training sequences, compare IAA with MP, OMP, and LSMP for channel estimation, and compare CLEAN-BLAST with RELAX-BLAST for symbol detection using simulations and/or the RACE'08 experimental results. Throughout this section, all the CIR estimation algorithms are followed by BIC to achieve sparsity.

A. Simulations

1. CIR estimation performance

To begin with, we consider the problem of CIR estimation for a 4×1 multi-input single-output (MISO) system with a time-invariant channel. The simulated CIR coefficients resemble real UWA conditions encountered in the RACE'08 experimental measurements. Figure 3 shows the modulus of the CIRs corresponding to the four transmitters where $R=30$ delay taps are considered. Given the training symbols, the received data samples are constructed using Eq. (5), where $\mathbf{e}_1$ is assumed to be a circularly symmetric independent and identically distributed (i.i.d.) complex-valued Gaussian random process with mean zero and variance σ^2.

Figure 4 shows the mean-squared error (MSE) of the channel estimates obtained by MP, OMP, LSMP, and IAA with two different training sequences: QPSK training and CA training. In QPSK training, each training symbol is randomly selected to be one of the four QPSK constellation points whereas in CA training each symbol is selected by using the CA algorithm described in Sec. III B. The training sequence length is set at $P=128$ symbols. Each point in Fig. 4 is obtained by averaging 100 Monte-Carlo trials. We observe that when the QPSK training is used, IAA significantly outperforms the other channel estimation methods. OMP and LSMP show similar performance whereas MP shows the worst performance. On the other hand, when the CA training sequences are used, the performance gap between IAA and the MP based channel estimation algorithms diminishes and all algorithms yield very similar performance although IAA still gives the lowest MSE. Moreover, the performance of IAA is not affected very much from the characteristics of the training sequences used. This is an advantage over the other methods since in the decision-directed mode, the channel has to be updated using the previously decoded symbols, which do not have as good auto- and cross-correlation properties as the specifically designed training sequences.

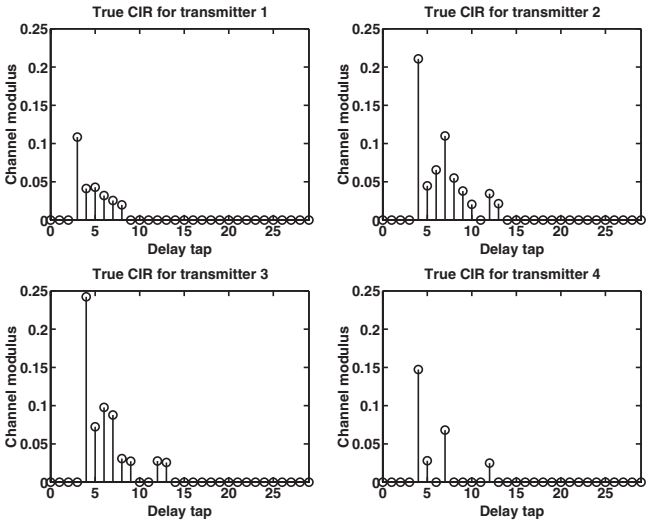

FIG. 3. The modulus of the simulated CIRs between the four transmitters and the receiver in a 4×1 MISO system.

2. Symbol detection performance

We now evaluate the bit error rates (BERs) of CLEAN-BLAST and RELAX-BLAST for a 4×12 MIMO system. The package structure shown in Fig. 1 is used in the simulations with CA training sequences consisting of $P=512$ symbols, a payload sequence consisting of 6000 QPSK modulated symbols, and two gaps consisting of 80 mute symbols each. IAA is used for channel estimation. The detection order for the algorithms is 3, 2, 4, and 1, i.e., the third channel is assumed to have the strongest channel response at all the receivers and the first channel the weakest. The average BERs over 100 Monte-Carlo trials are shown for the data transmitted from all four transducers in Fig. 5. We observe that RELAX-BLAST shows much better performance than

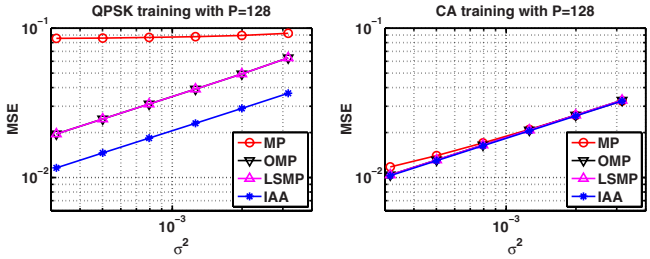

FIG. 4. (Color online) MSE of the CIR estimates for a 4×1 MISO system using the QPSK and CA training sequences with $P=128$ symbols. Each point is averaged over 100 Monte-Carlo trials.

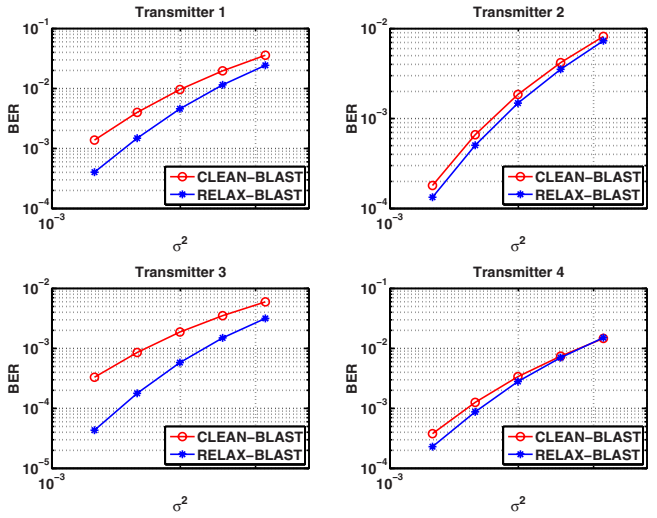

FIG. 5. (Color online) The BERs of each of the four transmitted payload sequences for a 4×12 MIMO system. The training sequences consist of $P=512$ symbols and are designed by the CA algorithm. The detection performance of CLEAN-BLAST and RELAX-BLAST is compared in terms of BER averaged over 100 independent Monte-Carlo trials for varying levels of the noise variance σ^2.

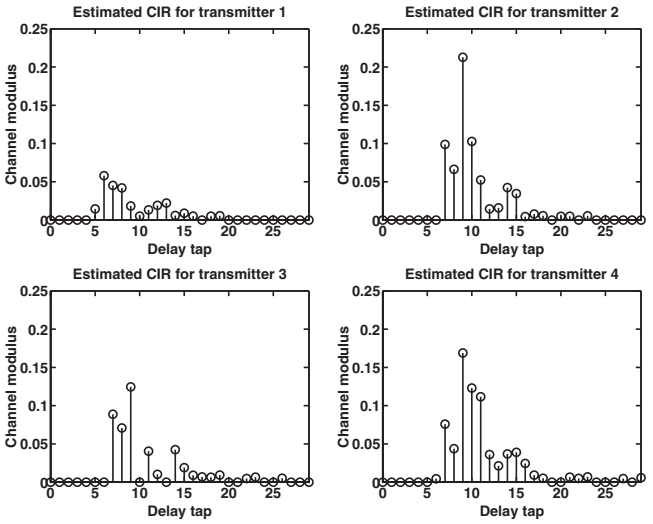

FIG. 6. The modulus of the four RACE'08 CIRs estimated by IAA for the first receiver from epoch "0830156".

CLEAN-BLAST as long as severe error propagation does not exist. This result is supported by the fact that similar performance improvements in spectral estimation are obtained when RELAX is used instead of CLEAN.[50,51] Due to this reason, we will use RELAX-BLAST when analyzing the RACE'08 data in the following.

B. RACE'08 experimental results

In this part, we evaluate our proposed MIMO underwater communications scheme using the RACE'08 experimental data set. RACE'08 was conducted by WHOI in Narragansett Bay. The water depths ranged from 9 to 14 m during the experiments. Surface conditions were primarily wind blown chop. A 4×24 MIMO system was used in the experiments. The primary transmitter was located approximately 4 m above the bottom of the ocean using a stationary tripod. Below the primary transmitter, a source array consisting of three transducers was deployed vertically with a spacing of 0.6 m between the elements. The top element of the source array was 1 m below the primary source. 24 receiving transducers were mounted at a range of approximately 400 m. Receivers were deployed vertically with a spacing of 0.05 m between the individual elements. The carrier frequency and the bandwidth employed in the RACE'08 experiments were 12 and 3.9 kHz, respectively.

The data packet that we will consider herein is from epoch "0830156". Some epochs could not be evaluated due to the severe conditions of sea. Among the many epochs that result in reasonable performance, epoch "0830156" was chosen arbitrarily. The package structure shown in Fig. 1 was used in the experiments with CA training sequences consisting of $P=512$ symbols, a payload sequence consisting of 2000 QPSK modulated symbols, and two gaps consisting of 80 mute symbols each. The symbol rate was 3906.25 symbols per second. By applying QPSK modulation and using four transmitters simultaneously, a 31.25 kbps uncoded payload data rate was achieved. The coding scheme we used for the experiments was a 1/2 convolutional encoder with constraint length of 5, and generator polynomials (1 0 0 1 1) and (1 1 0 1 1).[3] This coding scheme reduces the net payload data rate to 15.63 kbps.

The selection of the number of delay taps, R, to consider is very important. A value too small will loose important channel features whereas a value too large will complicate the receiver and may result in overfitting as well as increased noise. We found out empirically that $R=30$ yields reasonable results. Figure 6 shows the modulus of the training-directed IAA estimate of the CIR at receiver 1. The CIRs for the other receivers, i.e., $\{\hat{\mathbf{h}}_m\}_{m=2}^{24}$, share similar structure with $\hat{\mathbf{h}}_1$. As shown in Fig. 6, the detection order should be 2 (strongest coefficients), 4, 3, and 1 (weakest coefficients).

The channel tracking approach we follow is summarized in Fig. 7. In the first step, the CIR is estimated using the training sequences. Based on the initial CIR estimate, the first $L+50$ payload symbols are obtained using RELAX-BLAST, where L was defined after Eq. (8). Next, a decision-directed CIR estimation is done using the first L estimated symbols. The reason for not using all the $L+50$ estimated symbols will be explained shortly. With the updated CIR, starting from the $(L-49)$th symbol, the subsequent $L+100$ symbols are detected again using RELAX-BLAST. This process is repeated until all the 2000 payload symbols are detected. Figure 7 shows that 100 more symbols (50 more sym-

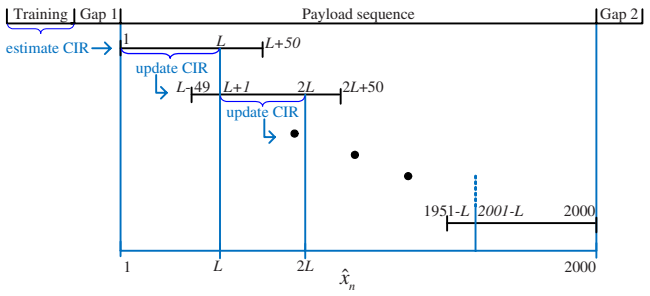

FIG. 7. (Color online) The channel tracking procedure.

TABLE IV. BER for $L=200$. Tx 1–4 stand for transmitters 1–4.

	Uncoded BER (%)				Coded BER (%)			
	Tx 1	Tx 2	Tx 3	Tx 4	Tx 1	Tx 2	Tx 3	Tx 4
MP	30.45	6.80	14.38	3.83	46.70	0	8.85	0
OMP	12.15	0.60	2.00	0.35	2.40	0	0	0
LSMP	12.15	0.60	2.00	0.35	2.40	0	0	0
IAA	4.63	0.10	0.35	0	0	0	0	0

bols at the first and last steps) are detected other than the L symbols used to update the CIR at each step. These 50 margin symbols on either end serve as guard intervals because the errors tend to happen at the beginning and end of each block. This is partly due to no mute symbols being available within the payload sequence.

In Table IV we show the uncoded and coded BERs obtained via MP, OMP, LSMP, or IAA as the channel estimation algorithm. For the results presented in this table, the number of payload symbols used for updating the channel coefficients is 200, i.e., $L=200$. We observe that IAA provides the best performance among all four algorithms. The average uncoded BER for IAA is 1.27%, MP is 13.86%, and OMP and LSMP is 3.78% and the coded average BER for IAA is 0%, MP is 13.89%, and OMP and LSMP is 0.6%. As expected, the sequence with the strongest (weakest) channel coefficients is estimated with the highest (lowest) accuracy, see Fig. 6.

In Table V the uncoded and coded BERs are shown for $L=400$. This means that the channel will be updated less frequently than in the case where $L=200$. We observe that now IAA, OMP, and LSMP show almost identical performance. The average uncoded BER for IAA is 0.38%, MP is 2.09%, and OMP and LSMP is 0.37% and the coded average BER for IAA is 0%, MP is 0.01%, and OMP and LSMP is 0%. As we mentioned previously, when L is large or the sequence used for updating the channel is well-structured, the performance of MP type of algorithms approaches that of IAA. However, it might not be always possible to select L large in practice.

The choice of L determines the rate at which the CIR will be updated in the decision-directed mode. It also determines the accuracy of the CIRs. As can be seen from Eq. (6), the larger the L, the more accurate the channel estimates will be assuming that the previously detected symbols are correct and the channel is stationary. On the other hand, for larger L, the channel will be updated less frequently and hence the results will be inaccurate for a rapidly varying channel. Therefore, the choice of L has a direct effect on the performances of MP, OMP, LSMP, and IAA. Moreover, L also determines the computational complexities of these algorithms. For the current set of data, we observed that the channel is rather benign and using a large L value results in better estimates than using a lower one, as seen in Tables IV and V. However, for a rapidly varying channel where L has to be selected small, IAA appears to be the best candidate for channel estimation as its performance is still good with small L whereas MP type of algorithms show relatively worse performance.

Note that in our experiments, neither the training sequence length P nor the gap lengths have been optimized for the best performance as no prior information of the experimental conditions was available. Moreover, for the current experimental conditions, a 1/2 rate convolutional code appears to be on the conservative side to achieve 0% coded BER.

VI. CONCLUSIONS

In this paper, we have focused on the various aspects of using a MIMO acoustic communications system in an underwater environment where delay spread is present. The problem was divided into two main parts: (i) channel estimation, which involves the design of the training sequences and the design of the algorithm to estimate the channel coefficients using the training sequences or previously detected symbols, and (ii) symbol detection. We have presented the CA for designing training sequences with good auto- and cross-correlation properties. IAA coupled with BIC and RELAX was presented as an approach for estimating the CIR. It was shown via simulations that IAA outperforms MP type of algorithms with arbitrary training sequences and it was shown

TABLE V. BER for $L=400$. Tx 1–4 stand for transmitters 1–4.

	Uncoded BER (%)				Coded BER (%)			
	Tx 1	Tx 2	Tx 3	Tx 4	Tx 1	Tx 2	Tx 3	Tx 4
MP	6.98	0.23	1.05	0.13	0.05	0	0	0
OMP	1.48	0	0	0	0	0	0	0
LSMP	1.48	0	0	0	0	0	0	0
IAA	1.50	0	0	0	0	0	0	0

via experimental data that IAA gives better results than MP type of algorithms when the number of symbols used for updating the channel is relatively small (a situation encountered in rapidly varying sea conditions). An extension to the widely used V-BLAST algorithm, namely, RELAX-BLAST, has been presented to improve detection performance. The validity of the proposed scheme was shown via both simulations and field data from the RACE'08 experiment.

ACKNOWLEDGMENTS

This work was supported in part by the Office of Naval Research (ONR) under Grant No. N00014-07-1-0193, the National Aeronautics and Space Administration (NASA) under Grant No. NNX07AO15A, and the National Science Foundation (NSF) under Grant No. ECS-0621879.

[1]J. Catipovic, "Performance limitations in underwater acoustic telemetry," IEEE J. Ocean. Eng. **15**, 205–216 (1990).
[2]J. Preisig, "Acoustic propagation considerations for underwater acoustic communications network development," ACM SIGMOBILE Mobile Computing Communications Review **11**, 2–10 (2007).
[3]J. G. Proakis, *Digital Communications*, 3rd ed. (McGraw-Hill, New York, NY, 1995).
[4]M. Stojanovic, J. Catipovic, and J. Proakis, "Phase-coherent digital communications for underwater acoustic channels," IEEE J. Ocean. Eng. **19**, 100–111 (1994).
[5]M. Chitre, S. Shahabudeen, and M. Stojanovic, "Underwater acoustic communications and networking: Recent advances and future challenges," Mar. Technol. Soc. J. **42**, 103–116 (2008).
[6]D. Kilfoyle and A. Baggeroer, "The state of the art in underwater acoustic telemetry," IEEE J. Ocean. Eng. **25**, 4–27 (2000).
[7]J. C. Preisig and G. B. Deane, "Surface wave focusing and acoustic communications in the surf zone," J. Acoust. Soc. Am. **116**, 2067–2080 (2004).
[8]D. J. Garrood, "Applications of the MFSK acoustic communications system," in Proceedings of the Oceans, Boston, MA (1981), pp. 67–71.
[9]A. Baggeroer, D. Koelsch, K. von der Heydt, and J. Catipovic, "DATS—A digital acoustic telemetry system for underwater communications," in Proceedings of the Oceans, Boston, MA (1981), pp. 55–60.
[10]E. Appleton, "Automatic synchronization of triode oscillators," Proc. Cambridge Philos. Soc. **21**, 231–248 (1922).
[11]G. Hsieh and J. Hung, "Phase-locked loop techniques—A survey," IEEE Trans. Ind. Electron. **43**, 609–615 (1996).
[12]T. H. Eggen, A. B. Baggeroer, and J. C. Preisig, "Communication over Doppler spread channels—Part I: Channel and receiver presentation," IEEE J. Ocean. Eng. **25**, 62–71 (2000).
[13]T. H. Eggen, J. C. Preisig, and A. B. Baggeroer, "Communication over Doppler spread channels—Part II: Receiver characterization and practical results," IEEE J. Ocean. Eng. **26**, 612–621 (2001).
[14]M. Stojanovic, "Recent advances in high-speed underwater acoustic communications," IEEE J. Ocean. Eng. **21**, 125–136 (1996).
[15]J. C. Preisig, "Performance analysis of adaptive equalization for coherent acoustic communications in the time-varying ocean environment," J. Acoust. Soc. Am. **118**, 263–278 (2005).
[16]D. R. Dowling, "Acoustic pulse compression using passive phase-conjugate processing," J. Acoust. Soc. Am. **95**, 1450–1458 (1994).
[17]T. C. Yang, "Temporal resolutions of time-reversal and passive-phase conjugation for underwater acoustic communications," IEEE J. Ocean. Eng. **28**, 229–245 (2003).
[18]T. C. Yang, "Differences between passive-phase conjugation and decision-feedback equalizer for underwater acoustic communications," IEEE J. Ocean. Eng. **29**, 472–487 (2004).
[19]M. Johnson, L. Freitag, and M. Stojanovic, "Improved Doppler tracking and correction for underwater acoustic communications," in IEEE International Conference on Acoustics, Speech, and Signal Processing, Munich, Germany (1997), Vol. **1**, pp. 575–578.
[20]L. Freitag, M. Johnson, and M. Stojanovic, "Efficient equalizer update algorithms for acoustic communication channels of varying complexity," in IEEE/MTS Oceans Conference (1997), Vol. **1**, pp. 580–585.
[21]T. C. Yang, "Channel Q function and capacity," in IEEE/MTS Oceans Conference (2005), Vol. **1**, pp. 273–277.
[22]T. C. Yang, "Correlation-based decision-feedback equalizer for underwater acoustic communications," IEEE J. Ocean. Eng. **30**, 865–880 (2005).
[23]T. C. Yang and A. Al-Kurd, "Performance limitations of joint adaptive channel equalizer and phase locking loop in random oceans: Initial test with data," in IEEE/MTS Oceans Conference (2000), Vol. **2**, pp. 803–808.
[24]T. Yardibi, J. Li, P. Stoica, M. Xue, and A. B. Baggeroer, "Source localization and sensing: A nonparametric iterative adaptive approach based on weighted least squares," IEEE Trans. Aerosp. Electron. Syst. (to be published).
[25]B. Song and J. Ritcey, "Spatial diversity equalization for MIMO ocean acoustic communication channels," IEEE J. Ocean. Eng. **21**, 505–512 (1996).
[26]S. Gray, J. Preisig, and D. Brady, "Multiuser detection in a horizontal underwater acoustic channel using array observations," IEEE Trans. Signal Process. **45**, 148–160 (1997).
[27]M. Nordenvaad and T. Oberg, "Iterative reception for acoustic underwater MIMO communications," in Proceedings of the Oceans, Boston, MA (2006), pp. 1–6.
[28]S. Roy, T. Duman, V. McDonald, and J. Proakis, "High-rate communication for underwater acoustic channels using multiple transmitters and space-time coding: Receiver structures and experimental results," IEEE J. Ocean. Eng. **32**, 663–688 (2007).
[29]D. Kilfoyle, J. C. Preisig, and A. B. Baggeroer, "Spatial modulation over partially coherent multiple-input/multiple-output channels," IEEE Trans. Signal Process. **51**, 794–804 (2003).
[30]D. Kilfoyle, J. C. Preisig, and A. B. Baggeroer, "Spatial modulation experiments in the underwater acoustic channel," IEEE J. Ocean. Eng. **30**, 406–415 (2005).
[31]W. Li and J. C. Preisig, "Estimation of rapidly time-varying sparse channels," IEEE J. Ocean. Eng. **32**, 927–939 (2007).
[32]H. Ryser, *Combinatorial Mathematics* (Wiley, New York, NY, 1963).
[33]W. Pratt, *Digital Signal Processing* (Wiley, New York, NY, 1978).
[34]S. Yang and J. Wu, "Optimal binary training sequence design for multiple-antenna systems over dispersive fading channels," IEEE Trans. Veh. Technol. **51**, 1271–1276 (2002).
[35]S. Wang and A. Abdi, "MIMO ISI channel estimation using uncorrelated Golay complementary sets of polyphase sequences," IEEE Trans. Veh. Technol. **56**, 3024–3039 (2007).
[36]P. Fan and W. H. Mow, "On optimal training sequence design for multiple-antenna systems over dispersive fading channels and its extensions," IEEE Trans. Veh. Technol. **53**, 1623–1626 (2004).
[37]J. Li, X. Zheng, and P. Stoica, "MIMO SAR imaging: Signal synthesis and receiver design," in The Second International Workshop on Computational Advances in Multi-Sensor Adaptive Processing, Saint Thomas, VI (2007), pp. 89–92.
[38]J. Li, P. Stoica, and X. Zheng, "Signal synthesis and receiver design for MIMO radar imaging," IEEE Trans. Signal Process. **56**, 3959–3968 (2008).
[39]B. K. Natarajan, "Sparse approximate solutions to linear systems," SIAM J. Comput. **24**, 227–234 (1995).
[40]S. Mallat and Z. Zhang, "Matching pursuits with time-frequency dictionaries," IEEE Trans. Signal Process. **41**, 3397–3415 (1993).
[41]S. F. Cotter, R. Adler, R. D. Rao, and K. Kreutz-Delgado, "Forward sequential algorithms for best basis selection," IEE Proc. Vision Image Signal Process. **146**, 235–244 (1999).
[42]W. Li, "Estimation and tracking of rapidly time-varying broadband acoustic communication channels," Ph.D. thesis, Massachusetts Institute of Technology, Cambridge, MA (2005).
[43]S. F. Cotter and B. D. Rao, "The adaptive matching pursuit algorithm for estimation and equalization of sparse time-varying channels," in 34th Asilomar Conference on Signals, Systems and Computers, Pacific Grove, CA (2000), Vol. **2**, pp. 1772–1776.
[44]S. F. Cotter and B. D. Rao, "Sparse channel estimation via matching pursuit with application to equalization," IEEE Trans. Commun. **50**, 374–377 (2002).
[45]M. Kocic, D. Brady, and M. Stojanovic, "Sparse equalization for real-time digital underwater acoustic communications," in IEEE/MTS Oceans Conference (1995), Vol. **3**, pp. 1417–1422.
[46]M. Stojanovic, L. Freitag, and M. Johnson, "Channel-estimation-based adaptive equalization of underwater acoustic signals," in IEEE/MTS Oceans Conference (1999), Vol. **2**, pp. 590–595.
[47]C. Carbonelli, S. Vedantam, and U. Mitra, "Sparse channel estimation with zero tap detection," in IEEE International Conference on Communications, Paris, France (2004), Vol. **6**, pp. 3173–3177.

[48]P. Stoica and Y. Selén, "Model-order selection: A review of information criterion rules," IEEE Signal Process. Mag. **21**, 36–47 (2004).
[49]G. Schwarz, "Estimating the dimension of a model," Ann. Stat. **6**, 461–464 (1978).
[50]J. Li and P. Stoica, "Efficient mixed-spectrum estimation with applications to target feature extraction," IEEE Trans. Signal Process. **44**, 281–295 (1996).
[51]J. Li, D. Zheng, and P. Stoica, "Angle and waveform estimation via RELAX," IEEE Trans. Aerosp. Electron. Syst. **33**, 1077–1087 (1997).
[52]R. L. Cupo, G. D. Golden, C. C. Martin, K. L. Sherman, N. R. Sollenberger, J. H. Winters, and P. W. Wolniansky, "A four-element adaptive antenna array for IS-136 PCS base stations," in 47th IEEE Vehicular Technology Conference (1997), Vol. **3**, pp. 1577–1581.
[53]P. W. Wolniansky, G. J. Foschini, G. D. Golden, and R. A. Valenzuela, "V-BLAST: An architecture for realizing very high data rates over the rich-scattering wireless channel," in Proceedings of the ISSSE, Pisa, Italy (1998), pp. 295–300.
[54]P. Stoica and R. L. Moses, *Spectral Analysis of Signals* (Prentice-Hall, Upper Saddle River, NJ, 2005).
[55]H. L. Van Trees, *Optimum Array Processing*, Detection, Estimation, and Modulation Theory (Wiley, New York, NY, 2002), Pt. IV.
[56]J. A. Högbom, "Aperture synthesis with a non-regular distribution of interferometer baselines," Astron. Astrophys. Suppl. Ser. **15**, 417–426 (1974).
[57]J. A. Tropp, I. S. Dhillon, R. W. Heath, and T. Strohmer, "Designing structured tight frames via an alternating projection method," IEEE Trans. Inf. Theory **51**, 188–209 (2005).
[58]R. A. Horn and C. R. Johnson, *Matrix Analysis* (Cambridge University Press, Cambridge, UK, 1985).
[59]P. Tsai, H. Kang, and T. Chiueh, "Joint weighted least-squares estimation of carrier-frequency offset and timing offset for OFDM systems over multipath fading channels," IEEE Trans. Veh. Technol. **54**, 211–223 (2005).
[60]T. Koike, "Optimum-weighted RLS channel estimation for time-varying fast fading MIMO channels," in IEEE International Conference on Communications, Glasgow, Scotland (2007), pp. 5015–5020.
[61]J. Li and P. Stoica, "An adaptive filtering approach to spectral estimation and SAR imaging," IEEE Trans. Signal Process. **44**, 1469–1484 (1996).
[62]P. Stoica, H. Li, and J. Li, "A new derivation of the APES filter," IEEE Signal Process. Lett. **6**, 205–206 (1999).
[63]P. Stoica, A. Jakobsson, and J. Li, "Matched-filter bank interpretation of some spectral estimators," Signal Process. **66**, 45–59 (1998).
[64]G. H. Golub and C. F. V. Loan, *Matrix Computations* (Johns Hopkins University Press, Baltimore, MD, 1989).
[65]N. Wiener, *Extrapolation, Interpolation, and Smoothing of Stationary Time Series* (Wiley, New York, NY, 1949).
[66]A. H. Sayed, *Fundamentals of Adaptive Filtering* (Wiley, New York, NY, 2003).
[67]U. Madhow and M. L. Honig, "MMSE interference suppression for direct-sequence spread-spectrum CDMA," IEEE Trans. Commun. **42**, 3178–3188 (1994).
[68]H. V. Poor and S. Verdú, "Probability of error in MMSE multiuser detection," IEEE Trans. Inf. Theory **43**, 858–871 (1997).
[69]U. J. Schwarz, "Mathematical-statistical description of the iterative beam removing technique (Method CLEAN)," Astron. Astrophys. **65**, 345–356 (1978).